The functionalization of graphene using electron-beam generated plasmas

M. Baraket,[1,a)] S. G. Walton,[1] E. H. Lock,[1] J. T. Robinson,[2] and F. K. Perkins[2]
[1]*Plasma Physics Division, Naval Research Laboratory, Washington, DC 20375, USA*
[2]*Electronics Division, Naval Research Laboratory, Washington, DC 20375, USA*

(Received 28 December 2009; accepted 14 April 2010; published online 8 June 2010)

A plasmas-based, reversible functionalization of graphene is discussed. Using electron-beam produced plasmas, oxygen and fluorine functionalities have been added by changing the processing gas mixtures from Ar/O_2 to Ar/SF_6, respectively. The reversibility of the functionalization was investigated by annealing the samples. The chemical composition and structural changes were studied by x-ray photoelectron spectroscopy and Raman spectroscopy. [doi:10.1063/1.3436556]

Graphene is a promising material for a variety of potential applications[1–5] due to its unique chemical and physical properties. However, adding functional groups, in controllable and reproducible ways, is of significant interest.[6,7] In this work, we demonstrate plasma-based functionalization of graphene, adding either oxygen or fluorine groups. The former was chosen because its addition offers the possibility of tuning the electrical properties from metallic to semiconductor.[8,9] Fluorine is interesting for a wide range of applications because its addition increases hydrophobicity,[10,11] reduces surface energy,[11] and is useful in bioapplications.[12] We also demonstrate a reduction back to graphene, through annealing, which helps better understand the chemistry of functionalization and damage-free desorption is critical in circuit printing[13] and energy storage applications.

Electron-beam generated plasmas produced in Ar/O_2 and Ar/SF_6 gas mixtures were used to introduce the above mentioned functionalities. The key attributes of electron-beam generated plasmas is that they offer high plasma densities (10^{10}–10^{11} cm^{-3}) along with low electron temperatures (<1 eV). As a result, large fluxes of low energy (<5 eV) ions are delivered to adjacent surfaces.[14] These features are particularly important in the processing of very thin and sensitive materials, such as graphene, since this technique allows the addition of functional groups without appreciable etching or altering the graphene lattice via ion bombardment. This is in stark contrast to most low-pressure discharges, where ion energies are typically well-above etching thresholds.

The experimental apparatus, shown in Fig. 1, has been described in detail elsewhere.[15] Pulsed, magnetically confined, high energy (2 keV) sheet electron-beams were injected into a diluted argon background to produce large area (60×25 cm^2) plasma sheets. The processing stage was located 2.5 cm from the electron-beam axis. The base pressure ($\sim10^{-7}$ Torr) in the chamber is maintained by a turbo molecular pump. The gases (Ar, O_2, and SF_6) were introduced through mass flow controllers and the desired operating pressures were achieved by throttling the turbo pump with a conductance limiter. The process parameters include a pressure of 50 mTorr Ar diluted with either O_2 or SF_6, where the reactive gas was 5% of the total flow rate. The plasma was operated at a duty factor of 10% (2 ms pulse width and 20 ms period) and the total treatment time was 60 s (plasma exposure time was 6 s). It should be noted that the plasma processing was performed at room temperature.

Graphene was produced by chemical vapor deposition growth on copper as described in Ref. 16. For O_2 functionalization, the copper substrate was retained for plasma treatment. For fluorination, the graphene was transferred to a Si/SiO_2 substrate, a common platform in device manufacturing, prior to plasma treatment. After treatment, the functionalized graphene samples were annealed in a rapid thermal annealing processing furnace (Axic, Inc.) at 500 °C in Ar (2 Torr) for 10 min. After each step, the chemical composition of the samples was identified by x-ray photoelectron spectroscopy (XPS, K-Alpha, Thermo scientific) and the structure of the samples were examined by Raman spectroscopy (Renishaw InVia Raman microscope).

The characteristics of pulsed, electron-beam generated plasmas containing O_2 (Ref. 17) and SF_6 (Ref. 18) are well documented. In both, ion energy measurements show a range of energies extending up to about 5 eV with a mean energy of approximately 3 eV, the latter is lower than the bonding energy of the C—C (3.6 eV) or C=C bonds (6.35 eV) that form the graphitic plane of graphene. In graphite, ion irradiation produces changes in the structure of the top layer such as lattice defects, amorphization, or swelling,[19] which will depend on the incident ion mass and energy. In the case

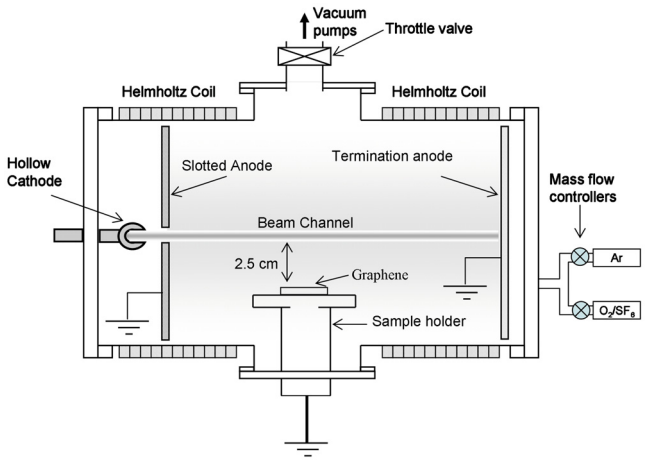

FIG. 1. (Color online) Schematic diagram of the plasma processing systems used in this work.

[a)]Author to whom correspondence should be addressed. NRC/NRL postdoctoral associate. Electronic mail: mira.baraket.ctr@nrl.navy.mil. FAX: +1 202 767 3553.

Author complimentary copy. Redistribution subject to AIP license or copyright, see http://apl.aip.org/apl/copyright.jsp

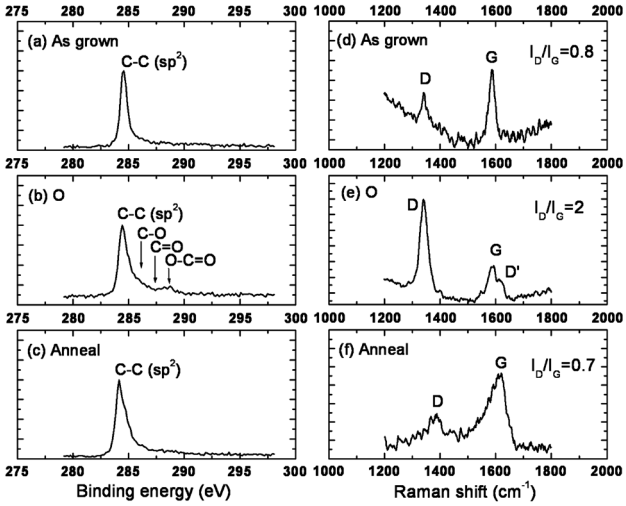

FIG. 2. C 1*s* high resolution XPS and Raman spectra of the [(a) and (d)] as-grown, [(b) and (e)] oxygenated, and [(c) and (f)] annealed oxygenated graphene, respectively.

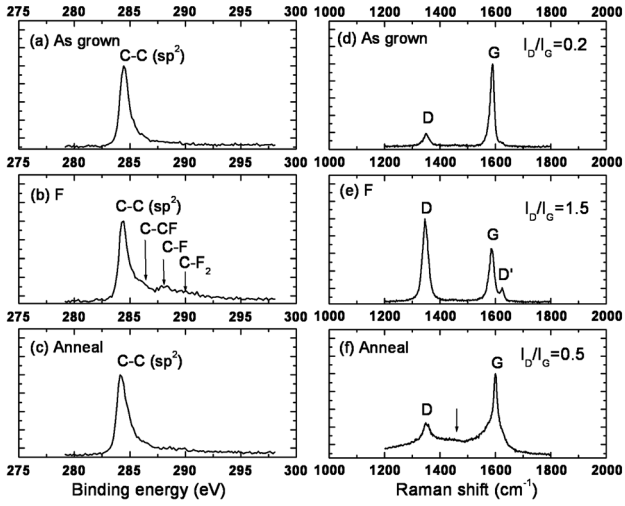

FIG. 3. C 1*s* high resolution XPS and Raman spectra of the [(a) and (d)] as-grown, [(b) and (e)] fluorinated, and [(c) and (f)] annealed fluorinated graphene, respectively.

of Ar^+ ions impacting graphite, the penetration and displacement thresholds have been estimated to be between 30 and 50 eV.[19,20] In our case, the ion energy is below 5 eV; well below the penetration and displacement thresholds of graphite and so no etching or changes in the lattice are expected from purely ballistic considerations.

While ion energies are low, the flux of reactive species in these systems is useful in producing the desired functionalities. In Ar/O_2, there is a large flux of O^+ ions and because electron–ion recombination proceeds rapidly in these plasmas, significant flux of reactive oxygen atoms is also expected. In the case of SF_6 containing plasmas, the primary ion species produced are SF_5^+ followed by SF_3^+. The creation of both ion species is accompanied by the production of reactive fluorine atoms. Thus, a wide range of reactions on the graphene surface to form either CO or CF_n functional groups is expected.

Chemical changes introduced via plasma treatment are easily observed by examining the XPS spectra of C 1*s* core level. The as-grown graphene exhibits the presence of C—C sp^2 bond at 284.4 eV [Figs. 2(a) and 3(a)]. The asymmetry in the peak is associated with the presence of oxygen (≈6 at. %) incorporated during handling and/or during transfer to the Si/SiO_2 substrate. After graphene is exposed to Ar/O_2 plasmas, the total oxygen concentration increases to 30 at. % (C/O=2.3). The presence of sp^2 C—C (284.4 eV), C—O (285.8 eV), C═O (287.3 eV), and O—C═O (288.6 eV) bonds can be identified in Fig. 2(b). After exposure to Ar/SF_6 plasmas, the total fluorine concentration is 18 at. % (C/F=4.5) and the C 1*s* spectra shows the incorporation of fluorinated functionalities as follows: C—CF (286.5 eV), C—F (288 eV), and C—F_2 (290 eV) bonds [Fig. 3(b)]. No sulfur or sulfur compounds were observed after treatment. Post-treatment washing with de-ionized water, produced no change in the XPS C 1*s* spectra, suggesting covalent bonding of fluorine to carbon.

In a perfect graphene layer, the six-membered hexagonal rings of carbon atoms are in the sp^2-hybridized state where each carbon atom is attached to three other carbon atoms. The Raman spectrum of the as-grown materials is characteristic of graphene. A G band, related to the vibrational modes in C_6 graphite rings, is observed around 1600 cm^{-1}. One does note the presence of a D band, which can arise from imperfections associated with discontinuities in the graphene film associated with the previously discussed handling/transfer. It is also worth noting the presence of a single G′ or 2D peak (not shown) around 2690 cm^{-1} with a full width at half-maximum of ≈35 cm^{-1}, which is characteristic of single layer graphene.[21,22]

A clear change in the Raman spectrum is seen after plasma treatment [Figs. 2(e) and 3(e)], most notably, the disorder-induced D peak intensity increased after functionalization [Figs. 2(e) and 3(e)] and surpassed the graphitic G band peak intensity (sp^2 mode). Although the incident ion energies are too low to cause impact-driven physical defects, the ion energies are sufficient to drive chemical reactions at the surface when reactive ions and/or neutrals are present during irradiation. When oxygen is incorporated, epoxy or ether groups are formed, where the C—C bonds undergo a change from sp^2 hybridization to distorted sp^3 hybridization. In the case of fluorine, two kinds of bonds with carbon are possible:[23] ionic bonds, which do not disturb the planar nature of the graphene and covalent bonds producing sp^3 hybridization. The increase in the intensity of the D band indicates a rising amount of the sp^3 bonded carbon in the modified-graphene structure caused by incorporated functionalities, observed by XPS. The intensity ratio of the D to G bands is an indicator of the degree of functionalization. These ratios are included in Figs. 2 and 3.

After annealing, the species adsorbed and the defects created by the functionalization are removed, as indicated in the XPS and Raman spectra shown in Figs. 2 and 3. Generally, the breadth of the C 1*s* peaks is reduced after annealing for both oxygen- and fluorine-functionalized graphene. In the case of fluorine functionalization, no fluorine was found in the annealed sample. From the Raman spectra, the D and D′ peak intensities decreased drastically as do the D to G intensity ratios.

On the other hand, a broadening and a symmetry loss of the D and G peaks, after annealing, are observed when compared to the as-grown graphene. In the fluorine-modified graphene, the presence of a broad band around 1450 cm^{-1}

Author complimentary copy. Redistribution subject to AIP license or copyright, see http://apl.aip.org/apl/copyright.jsp

[see arrow in Fig. 3(f)] related to amorphous[24] or disordered graphite[25] is also observed. Both attributes could be associated with vacancies and disordered carbon atoms[26] created in the graphitic structure by desorption of carbon containing functionalities. Desorption from oxygen-modified graphene may occur in the form of CO, CO_2, or H_2O,[27] and desorption from fluorine-modified graphite is known to occur in the form of CF_n compounds.[28,29]

In graphite, the recovery process, upon annealing, can be remarkably different depending on the ion irradiation dose/energy.[30] In this work, the recovery is certainly due to the low-energy ion flux during functionalization, which produces no major sputtering or carbon desorption. While bending and breaking of the carbon bonds are likely, they occur without major changes in the long range order of the graphite structure. Indeed, the defects recover easily at relatively low annealing temperatures of 500 °C.

In summary, electron-beam generated plasmas produced in different gas mixtures were used to add functionalities to graphene. Oxygen, using Ar/O_2 mixtures, and fluorine, using Ar/SF_6 mixtures, functional groups were added to graphene and then removed via annealing. The addition and subtraction of these functional groups occur without any significant unwanted or permanent changes to the underlying graphene structure. Based on these results, it is assumed that a broad range of functionalities maybe added by simply varying the operating gas and is currently being pursued. Although further characterizations of these materials, as they relate to device integration, are needed, the use of electron-beam generated plasmas, characterized by low ion energies, to functionalize graphene represents an attractive pathway to industrial scale fabrication.

This research was supported by the Office of Naval Research. M.B. appreciates the support of the National Research Council.

[1]Z. F. Wang, H. Zheng, Q. W. Shi, and J. Chen, ACM J. Emerg. Technol. Comput. Syst. **5**, 1 (2009).
[2]G. Eda, G. Fanchini, and M. Chhowalla, Nat. Nanotechnol. **3**, 270 (2008).
[3]N. Chopra, L. G. Bachas, and M. R. Knecht, Chem. Mater. **21**, 1176 (2009).
[4]C. Shan, H. Yang, J. Song, D. Han, A. Ivaska, and L. Niu, Anal. Chem. **81**, 2378 (2009).
[5]Y. Xu, L. Zhao, H. Bai, W. Hong, C. Li, and G. Shi, J. Am. Chem. Soc. **131**, 13490 (2009).
[6]D. W. Boukhvalov and M. I. Katsnelson, J. Phys.: Condens. Matter **21**, 344205 (2009).
[7]J. Dai, J. Yuan, and P. Giannozzi, Appl. Phys. Lett. **95**, 232105 (2009).
[8]I. Jung, D. Dikin, S. Park, W. Cai, S. L. Mielke, and R. S. Ruoff, J. Phys. Chem. C **112**, 20264 (2008).
[9]I. Jung, D. A. Dikin, R. D. Piner, and R. S. Ruoff, Nano Lett. **8**, 4283 (2008).
[10]R. Hatada and K. Baba, Nucl. Instrum. Methods Phys. Res. B **148**, 655 (1999).
[11]L.-Y. Meng and S.-J. Park, J. Colloid Interface Sci. **342**, 559 (2010).
[12]R. Hauert, U. Muller, G. Francz, F. Birchler, A. Schroeder, J. Mayer, and E. Wintermantel, Thin Solid Films **308–309**, 191 (1997).
[13]P. Sessi, J. R. Guest, M. Bode, and N. P. Guisinger, Nano Lett. **9**, 4343 (2009).
[14]S. G. Walton, C. Muratore, D. Leonhardt, R. F. Fernsler, D. D. Blackwell, and R. A. Meger, Surf. Coat. Technol. **186**, 40 (2004).
[15]D. Leonhardt, S. G. Walton, and R. F. Fernsler, Phys. Plasmas **14**, 057103 (2007).
[16]X. Li, W. Cai, J. An, S. Kim, J. Nah, D. Yang, R. Piner, A. Velamakanni, I. Jung, E. Tutuc, S. K. Banerjee, L. Colombo, and R. S. Ruoff, Science **324**, 1312 (2009).
[17]S. G. Walton, D. Leonhardt, D. D. Blackwell, R. F. Fernsler, D. P. Murphy, and R. A. Meger, Phys. Rev. E **65**, 046412 (2002).
[18]S. G. Walton, E. H. Lock, and R. F. Fernsler, Plasma Processes Polym. **5**, 453 (2008).
[19]D. Marton, K. J. Boyd, T. Lytle, and J. W. Rabalais, Phys. Rev. B **48**, 6757 (1993).
[20]J. R. Hahn, H. Kang, S. Song, and J. C. Jeon, Phys. Rev. B **53**, R1725 (1996).
[21]A. C. Ferrari, J. C. Meyer, V. Scardaci, C. Casiraghi, M. Lazzeri, F. Mauri, S. Piscanec, D. Jiang, K. S. Novoselov, S. Roth, and A. K. Geim, Phys. Rev. Lett. **97**, 187401 (2006).
[22]D. Graf, F. Molitor, K. Ensslin, C. Stampfer, A. Jungen, C. Hierold, and L. Wirtz, Nano Lett. **7**, 238 (2007).
[23]T. Nakajima, *Fluorine-Carbon and Fluoride-Carbon Materials* (Marcel Dekker, New York, 1994).
[24]R. N. Tarrant, O. Warschkow, and D. R. McKenzie, Vib. Spectrosc. **41**, 232 (2006).
[25]F. C. Tai, S. C. Lee, J. Chen, C. Wei, and S. H. Chang, J. Raman Spectrosc. **40**, 1055 (2009).
[26]A. C. Ferrari and J. Robertson, Phys. Rev. B **61**, 14095 (2000).
[27]I. Jung, D. A. Field, N. J. Clark, Y. Zhu, D. Yang, R. D. Piner, S. Stankovich, D. A. Dikin, H. Geisler, C. A. Ventrice, Jr., and R. S. Ruoff, J. Phys. Chem. C **113**, 18480 (2009).
[28]N. Watanabe and S. Koyama, Bull. Chem. Soc. Jpn. **53**, 3093 (1980).
[29]N. Watanabe, T. Kawamura, and S. Koyama, Bull. Chem. Soc. Jpn. **53**, 3100 (1980).
[30]K. Niwase, T. Tanabe, and I. Tanaka, J. Nucl. Mater. **191–194**, Part 1, 335 (1992).

Author complimentary copy. Redistribution subject to AIP license or copyright, see http://apl.aip.org/apl/copyright.jsp